Visualization study of thermal counterflow of superfluid helium in the proximity of the heat source by using solid deuterium hydride particles

P. Švančara, P. Hrubcová, M. Rotter, and M. La Mantia[*]

Faculty of Mathematics and Physics, Charles University, Ke Karlovu 3, 121 16 Prague, Czech Republic

Steady-state thermal counterflow of superfluid ^{4}He (He II) is experimentally investigated in a channel of square cross section, with a planar heater placed at its bottom. We focus on the flow region close to the heat source, which has received little attention to date. Relatively small particles of solid deuterium hydride, having a density comparable to that of He II, are suspended in the liquid and their flow-induced dynamics is studied by using the particle tracking velocimetry technique. The comparison with results obtained in similar conditions with solid deuterium particles, which are about 1.4 times denser than He II, confirms that, in the heater proximity, the mean distance between quantized vortices, representing the characteristic length scale of the flow, appears to be about one order of magnitude smaller than that expected in the bulk, at the same temperature and applied heat flux. Additionally, we find that the lighter particles seem to experience a slightly denser vortex tangle, supporting therefore the view that heavy particles tend to stay trapped on quantized vortices for longer times than light ones. In the range of investigated parameters, the heavier particles consequently appear to be more suitable to probe the occurrence of vortex reconnections, deemed to be crucial in explaining energy dissipation mechanisms in quantum flows.

I. INTRODUCTION

The study of superfluid ^{4}He (He II) belongs to the active and challenging research field focusing on the investigation of quantum turbulence [1–4] and combines classical fluid mechanics with quantum physics. This unique liquid can be described, on the phenomenological level, as a mixture of two fluids. The viscous (normal) component is viewed as the carrier of the liquid entropy, while the superfluid component is assumed inviscid and the circulation of its velocity is quantized, allowing thus the existence of tiny quantum vortices, of angstrom size, usually arranged in a tangle.

Above 1 K, as in the present study, the density ratio of the two components depends steeply on temperature, i.e., in close proximity to the superfluid transition temperature (2.17 K, at the saturated vapor pressure) the fluid is modeled solely by the normal component, while below 1 K the liquid can be said to be entirely superfluid. Additionally, the interaction between the components is ensured by the presence of the quantized vortex tangle. Turbulent flows of He II may therefore display features that are absent in classical turbulent flows of viscous fluids but, at the same time, are also characterized by classical-like properties (see, e.g., Ref. [5] and references therein).

Indeed, similarities and differences between quantum and classical flows have yet to be entirely understood, and in recent years they have been the focus of several studies, stimulated by the application of classical visualization techniques to flows of He II [6]. It has been shown clearly that the motions of relatively small particles in turbulent flows of superfluid ^{4}He display quantum

---

*lamantia@nbox.troja.mff.cuni.cz

features at scales smaller than the mean distance ℓ between quantized vortices [7], while at larger scales a classical-like picture emerges, at least if one considers the Lagrangian measurements performed to date [5].

In the Eulerian case the situation is instead less clear because some numerical simulations (see, e.g., Ref. [8]) suggest that, at scales larger than ℓ, the fluid velocity structure functions should display features not observed in classical turbulence and due consequently to the quantum nature of the studied flows. However, this is yet to be neatly observed experimentally as, for example, Rusaouen *et al.* [9] reported recently that, for a mechanically driven turbulent flow of He II, the scaling exponents of the Eulerian structure functions behave classically at scales appreciably larger than ℓ.

The present experimental study addresses, from the Lagrangian viewpoint, two other unresolved problems in quantum turbulence research, related, nevertheless, to the current quest for classical-like features of turbulent flows of superfluid ^{4}He. One concerns the influence of solid boundaries on the development of quantum flows, which is yet to be clarified [10–12], and the other focuses on the flow-induced behavior of small particles suspended in He II, which similarly has been mostly investigated by numerical means [13,14].

In our recent experiments [11] we suspended small deuterium particles in the liquid and studied by visualization the corresponding flow-induced dynamics in proximity to the flow source. Here we investigate the same quantum flow, in similar conditions, but we use lighter particles, made of solid deuterium hydride, and perform relevant comparison with our previous results in order to understand how particle inertia may influence the observed behavior, that is, the statistical distributions of the particle velocities.

The investigated flow, thermal counterflow, can be regarded as the most studied type of superfluid ^{4}He flow (see, e.g., Ref. [4]) and is here generated by a planar heater placed at the bottom of a vertical channel of square cross section. It can be said that, once the heater (the flow source) is switched on, the fluid components move on average in opposite directions, i.e., the normal fluid upward and the superfluid towards the heat source.

The flow-induced particle motions are captured by employing the particle tracking velocimetry technique [6] and we can then compute the corresponding velocity statistical distributions, which are characterized by power-law tails at scales smaller than ℓ [15]. These quantum tails gradually disappear as the scale probed by the particles increases until the distribution form becomes nearly Gaussian, i.e., classical-like [16], at scales larger than the mean distance between quantized vortices. It is consequently possible to estimate the flow characteristic scale ℓ by looking at the distribution shape (i.e., at its flatness) as a function of the probed scale [11,17].

As mentioned above, only recently, a number of studies have been dedicated to the effect of solid boundaries on the development of quantum flows (see, for example, Ref. [11] and references therein) and the main result, which applies to various types of He II flows, is that boundary layers may also exist in quantum flows, although their origin seems to be related more to the quantized vortex dynamics than to the fluid viscosity. Additionally, Hrubcová *et al.* [11] have investigated by visualization the thermal counterflow behavior in close proximity to the heater, the solid boundary perpendicular to the mean flow direction, and the main outcome (obtained by using solid deuterium particles) is that the vortex tangle appears to be significantly denser close to the heater than in the bulk, at least in the range of investigated parameters.

We then decided to perform another series of experiments, in similar conditions, by using different particles. We wanted to observe again the significant decrease of the characteristic scale ℓ close to the heater by using other probes (in order to confirm our previous finding) and, at the same time, we wanted to investigate the effect of the particle inertia on the studied flow-induced dynamics. The latter topic, as mentioned above, is yet to be extensively addressed in quantum turbulence research, while the study of particle dynamics in classical turbulent flows has a long history [18,19]. By investigating how particles behave in quantum flows and by performing relevant comparisons with what has been observed in particle-laden flows of viscous fluids, it is indeed

possible to take part in the current quest for large-scale quantum features of turbulent flows of He II [5,7].

The present work belongs to this scientific line of enquiry. On the one hand, from experimental data, including those presented below, it can be argued that, in the range of investigated parameters, the mean distance between quantized vortices is, close to the heater, approximately one order of magnitude smaller than that expected in the bulk, at the same temperature and applied heat flux. On the other hand, the precise value of the observed ℓ decrease appears to depend on the particle inertia, which nevertheless seems to have a less significant influence on the corresponding flow-induced dynamics than the boundary proximity.

The reader should however keep in mind that the present study focuses more on the dynamics of different particles in the same quantum flow than on the fact that thermal counterflow is being investigated close to the heater, which was instead the main focus of our recent publication [11]. Indeed, as detailed below, we specifically discuss here how our visualization results can be explained on the basis of the particle inertia and how the experimental conditions, i.e., temperature and applied heat flux, may affect the flow-induced particle motions and therefore justify the obtained experimental findings.

II. METHODS

The experimental setup and data processing procedure have already been described in Ref. [11]. We therefore highlight in the following solely the methods relevant to the present work.

In previous experiments the particles suspended in the liquid were made of solid deuterium D (or hydrogen H) and their mean size was a few micrometers (see Refs. [5,15] for typical particle-size distributions). Here we instead employ solid deuterium hydride HD, which has a density comparable to that of the liquid, i.e., $\rho_{HD} \approx 145$ kg/m^3, while $\rho_H \approx 88$ kg/m^3 and $\rho_D \approx 200$ kg/m^3; estimates are made starting from the crystal structure parameters reported in Ref. [20].

It follows that, in the same quantum flow, solid deuterium particles ought to accelerate less than He II, while the opposite applies to hydrogen particles [14]. In the case of deuterium hydride it is instead expected that the solid particle acceleration is almost equal to that of the liquid. For this reason we did not estimate the mean size of HD particles from corresponding free-fall velocities [21], but we looked at the apparent particle size in movies taken in similar experimental conditions. We found that HD and D particles have on average the same brightness on the images and we therefore assume that deuterium hydride particles have dimensions comparable to those of the others.

We generated the particles by using the same procedure employed in the past, i.e., we suitably mixed helium and HD gases at room temperature and we then injected the mixture into the helium bath. It is therefore useful to remark that HD gas contains significant amounts of hydrogen and deuterium molecules and that the equilibrium ratio between the three substances depends on temperature [22]. For example, it can be estimated that, at room temperature, approximately half of the volume consists of H and D molecules. It follows that any HD gas volume is actually a mixture of H, D, and HD molecules (this explains why, in the absence of any flow, we could see, in the helium bath, particles moving upward and downward).

Note also that reports of the use of HD particles for the visualization of He II flows are lacking (see, for example, Ref. [6] and references therein). This might appear surprising if one considers that the density of solid deuterium hydride is almost equal to that of He II and that consequently small enough HD particles could in principle be perfect tracers for liquid helium flows. However, as shown above, it is not possible in the current setup to obtain a volume of HD gas that does not include hydrogen and deuterium molecules.

Other experimental details, such as the employed particle tracking algorithm [23], are reported in Ref. [11]. For the sake of clarity, we recall here that images are collected approximately 1 mm above the planar heater (the square channel has 25 mm sides and is 10 cm high) and that our camera field of view (13 mm wide and 8 mm high) is situated in the middle of the channel, as far away as

possible from its vertical walls. Note, additionally, that, in the case of the bulk experiments [7], also employed in the following as a term of comparison, the field of view is located about 5 cm (two hydraulic diameters [24]) above the flow source.

In order to understand the obtained results it is now useful to recall the definitions of some relevant quantities. We start from the scale s_p probed by the particles, estimated as the mean particle velocity V multiplied by the time t between two consecutive positions, where V has been obtained at the smallest t, which is 2.5 ms (2 ms) for bulk (heater proximity) cases. We find that its smallest values range from 3 to 10 μm, that is, they are of the same order as the mean particle size. Note also that s_p can be increased by removing particle positions from the trajectories obtained at the smallest time [15].

The scales probed by the particles then have to be compared to the characteristic scale of the flow, i.e., the mean distance ℓ between quantum vortices, which, for He II flows, is often set equal to $1/\sqrt{L}$, where the vortex line density L denotes the total length of quantized vortices per unit volume. The latter quantity depends on the flow type and, in the case of thermal counterflow, it is generally assumed that, in the bulk, L is proportional to the square of the counterflow velocity v_{ns}, which characterizes each experimental run. This velocity is defined as

$$v_{ns} = v_n - v_s = \frac{q}{\rho S T}\left(1 + \frac{\rho_n}{\rho_s}\right) = \frac{q}{\rho_s S T}, \tag{1}$$

where v_n and v_s indicate the mean normal fluid and superfluid velocities, respectively (we assume that $v_n > 0$ and $v_s < 0$), and q denotes the applied heat flux; the total density ρ of the fluid, which depends weakly on the liquid temperature T, is equal to the sum of the T-dependent densities of its normal (ρ_n) and superfluid (ρ_s) components, and S denotes the entropy per unit mass, tabulated, together with other fluid properties, in Ref. [25]. By using v_{ns} it is also possible to define the Reynolds number

$$\text{Re} = \frac{\rho v_{ns} D}{\mu}, \tag{2}$$

where $D = 25$ mm indicates the channel hydraulic diameter and μ denotes the dynamic viscosity of the He II normal component, which is also tabulated in Ref. [25]. Note that for the present channel the turbulence onset occurs at Re ≈ 2300, corresponding to $v_{ns} \approx 1$ mm/s [24].

We can now return to the definition of the characteristic length scale of the flow and, following the previous reasoning, we can write

$$\ell = 1/\gamma v_{ns}, \tag{3}$$

where the parameter γ depends on T (see, for example, Ref. [26] for a discussion on this quantity). For the sake of consistency with Ref. [11], we also employ here the γ values reported in Ref. [27]; these values were taken (and interpolated) from a table in Ref. [28] and they were computed by using the numerical results obtained by Schwarz [29] for homogenous turbulence, i.e., in the bulk (see also Ref. [30]).

As mentioned above, we calculate, for each experimental condition, the statistical distribution of the particle velocities and in order to further characterize our observations we use the scale ratio

$$R = \frac{s_p}{\ell} = \frac{Vt}{\ell} = \frac{t}{\tau} = (\gamma v_{ns} V)t, \tag{4}$$

where t indicates the time between consecutive particle positions and the characteristic time

$$\tau = 1/\gamma v_{ns} V. \tag{5}$$

The free parameter in Eq. (4) is the time, once T, q, and particle type are given. It then follows that, by removing particle positions from the tracks computed at the smallest time, i.e., by increasing t in Eq. (4), it is possible to access larger flow scales. As shown below, in the range of investigated parameters, we can probe scales straddling about two orders of magnitude across ℓ.

TABLE I. Experimental conditions for BH, bulk thermal counterflow, with hydrogen particles; BD, bulk thermal counterflow, with deuterium particles; D1–D4, thermal counterflow in the heater proximity, with deuterium particles; and HD1–HD4H, thermal counterflow in the heater proximity, with deuterium hydride particles. The parameters are temperature T, applied heat flux q, thermal counterflow velocity v_{ns} [Eq. (1)], Reynolds number Re [Eq. (2)], mean particle velocity V at the smallest time t between particle positions, characteristic length scale ℓ [Eq. (3)], and characteristic time τ [Eq. (5)].

Case	T (K)	q (W/m^2)	v_{ns} (mm/s)	Re/10^3	V (mm/s)	ℓ (μm)	τ (ms)
BH	1.77	612	6.8	19.0	2.4	70	29
BD	1.77	608	6.7	18.8	3.9	70	18
D1	1.24	23	2.2	4.0	2.2	674	305
D2	1.40	54	2.2	5.2	2.4	409	168
D3L	1.75	235	2.7	7.6	2.3	177	76
D3H	1.75	417	4.9	13.5	3.5	100	29
D4	1.95	234	1.9	5.1	1.6	183	113
HD1	1.24	20	1.9	3.5	1.7	770	459
HD2L	1.40	25	1.0	2.5	1.5	868	598
HD2M	1.40	48	2.0	4.7	1.8	455	256
HD2H	1.40	65	2.6	6.3	2.3	338	148
HD4L	1.95	200	1.7	4.3	1.6	214	135
HD4H	1.95	779	6.5	16.9	5.4	55	10

In Table I the experimental conditions are summarized. It is apparent that the calculated characteristic length scales are appreciably larger than the minimum values of s_p, which, as reported above, range between 3 and 10 μm. Additionally, the computed characteristic times are larger than the smallest times between frames, equal to 2.5 ms (2 ms) for bulk (heater proximity) cases. Note that the data sets BH, BD, D1, D2, D3L, and D4 have already been employed in Ref. [11] and that here they are solely used as terms of comparison, i.e., to highlight the findings we obtained by probing thermal counterflow with HD particles.

Finally, we assume that the studied flows have reached the steady state because the movies were collected at least a few seconds after the heater was switched on and, as discussed in Ref. [11], relevant diffusion times can be estimated (to a first approximation, following Ref. [31]) to be orders of magnitude smaller than the time we waited before taking the movies, at least in the range of investigated temperatures and applied heat fluxes. The assumption is also supported if we calculate, in the present conditions, the kinetic time, introduced in Ref. [32] and defined as the time it takes for the fluid to gain the kinetic energy supplied by the heater. Indeed, corresponding values are found to be of the same order as the problem diffusion times.

III. RESULTS AND DISCUSSION

For the sake of comparison, we present our results in the same fashion as in Ref. [11]. We plot in Fig. 1 the normalized fourth moment of the particle velocity distribution, i.e., its flatness, as a function of the scale ratio R (the flatness of the standard Gaussian distribution is equal to 3).

As discussed in Ref. [7], the relatively large flatness values observed at the smallest scales are due to the distribution power-law tails, which can be explained by taking into account the interactions between particles and quantized vortices. Additionally, for the bulk cases, it has been reported several times that, at scales larger than ℓ, for $R \geqslant 1$, the distribution shape is classical-like, i.e., it has a nearly Gaussian form [16].

It is evident from Fig. 1 that the flatness trends obtained with HD particles broadly confirm the significant enhancement of vortex line density observed in the heater proximity by using deuterium
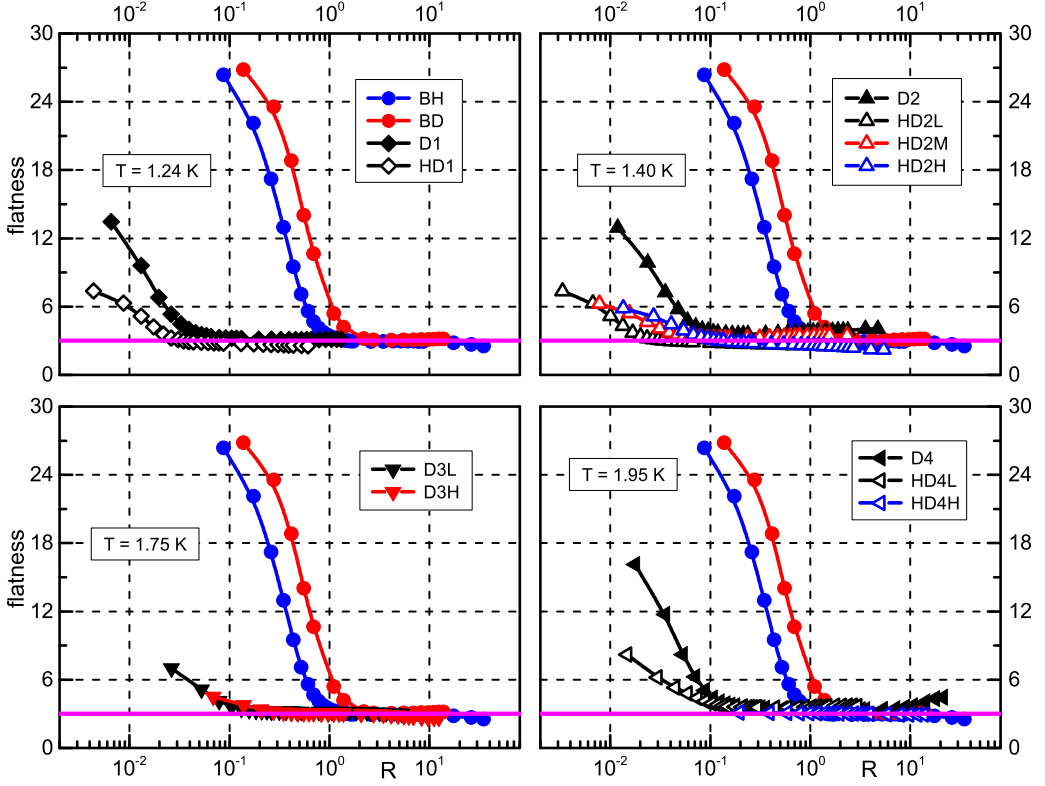
FIG. 1. Flatness of the $(u - u_m)/u_{\text{s.d.}}$ distribution as a function of the scale ratio R [Eq. (4)], where u_m and $u_{\text{s.d.}}$ indicate the mean value and the standard deviation of the instantaneous dimensional velocity u in the horizontal direction, respectively (u is positive if directed from the left to the right of the field of view); at least 10^5 velocities are taken into account for each R. Circles denote counterflow data obtained in the bulk; closed and open symbols indicate data obtained in the heater proximity with deuterium and deuterium hydride particles, respectively; see Table I for the experimental conditions (the data sets are labeled accordingly in the figure; the temperature of the heater proximity cases is specified in each panel; the bulk data were obtained at 1.77 K). The magenta line shows the flatness of the Gaussian distribution.

probes [11], that is, they also indicate that the characteristic length scales estimated by using Eq. (3) might not be the correct ones close to the flow source. In the following we discuss (i) how particle inertia can be employed to explain the obtained results and (ii) how the apparent increase of vortex line density in the heater proximity may depend on temperature and applied heat flux.

Indeed, as shown in Fig. 2, the calculated flatness values are appreciably influenced by the experimental conditions, i.e., temperature, applied heat flux, and particle type, although it is difficult to deny that particles appear to experience in the heater proximity vortex tangles denser than in the bulk.

A. Particle inertia

We also use here, as in Ref. [11], the effective scale ratio

$$R_1 = cR = c(\gamma v_{ns} V)t, \qquad (6)$$

where the parameter c can be regarded as a first-order estimate of the observed ℓ decrease and, following Ref. [11], we take the BH data set (corresponding to bulk thermal counterflow with hydrogen particles) as the reference case because its flatness reaches the Gaussian value at $R \approx 1$.
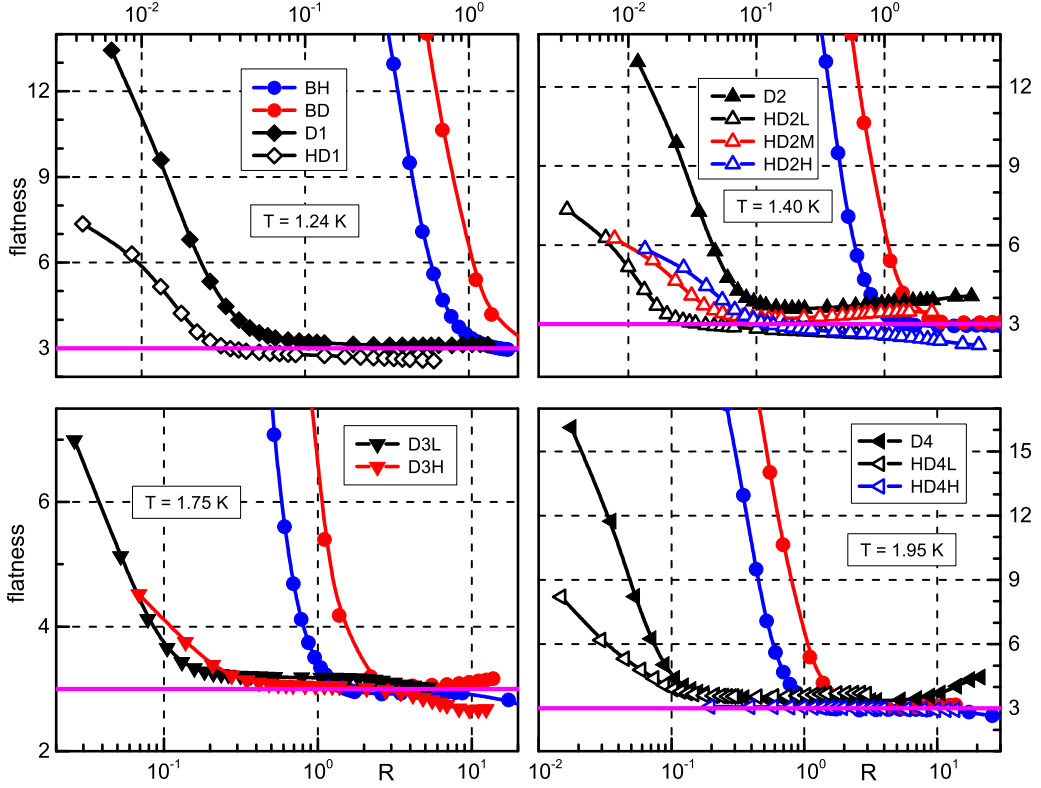
FIG. 2. Flatness of the $(u - u_m)/u_{\text{s.d.}}$ distribution as a function of the scale ratio R [Eq. (4)]. The symbols have the same meaning as in Fig. 1 (see also Table I). Note that, compared to Fig. 1, different scales are used here to highlight the data obtained in the heater proximity.

We display in Fig. 3 the velocity distribution flatness as a function of R_1 and show the same data in Fig. 4 by using different scales in order to highlight the particle behavior close to the heater. It is apparent that the c bulk values are about one order of magnitude smaller than those found in the heater proximity (the reason why we set $c = 1$ for the HD4H case is addressed below).

We can also notice in Fig. 3 that the c value obtained in the bulk with deuterium particles (BD) is half of that with hydrogen particles. As already pointed out in Ref. [17], this can be explained by taking into account the fact that hydrogen particles ought to accelerate about two times more than deuterium ones [14]. Indeed, following Ref. [14], we can write

$$\frac{d\mathbf{u}_p}{dt} = \frac{1 + C}{\rho_p/\rho_f + C} \frac{D\mathbf{u}_f}{Dt} = K_p \frac{D\mathbf{u}_f}{Dt}, \tag{7}$$

where $\mathbf{u}_p$ indicates the instantaneous velocity vector of a (small enough) particle p in a fluid f, characterized by the instantaneous velocity vector $\mathbf{u}_f$, and C is known as the added mass coefficient, equal to 1/2 for a spherical particle; ρ_p and ρ_f denote the particle and fluid density, respectively, $D\mathbf{u}_f/Dt$ indicates the Lagrangian derivative of the fluid velocity, and K_p can be seen as the ratio between particle and fluid accelerations.

We consequently obtain that, for spherical particles accelerating in He II, $K_H/K_D \approx 1.70$ and $K_{HD}/K_D \approx 1.25$, where the subscript indicates the particle type. The finding is consistent with the flatness trends shown in Fig. 3 if one compares flows having similar temperature and applied heat flux but probed by using different particles, i.e., BH with BD, HD1 with D1, HD2M with D2, and HD4L with D4. We specifically find that in the heater proximity $c_{HD}/c_D \approx 2$, similarly to what is
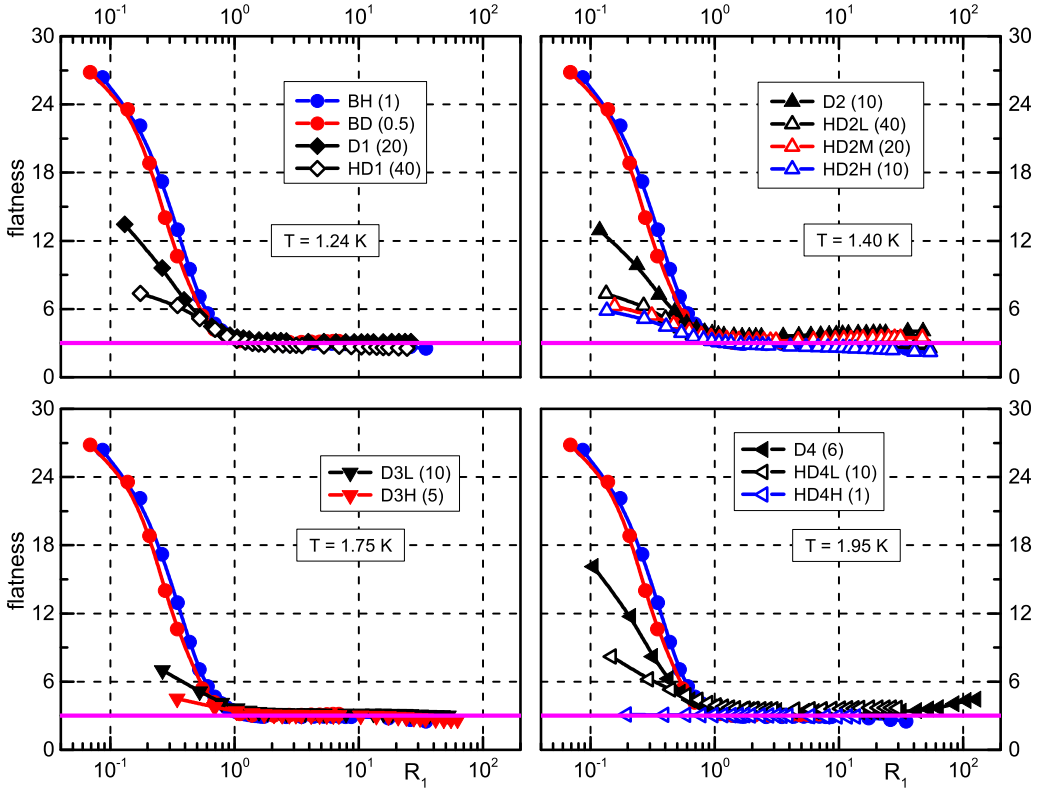
FIG. 3. Flatness of the $(u - u_m)/u_{\text{s.d.}}$ distribution as a function of the effective scale ratio $R_1 = cR$ [Eq. (6)]. Relevant c values are shown in parentheses following the data set symbols, which are as in Fig. 1 (see also Table I).

observed in the bulk when one compares BH with BD [17], which also means that light particles tend to accelerate more than heavy ones regardless of the flow region being investigated.

Considering that our particles are generally not spheres [21] and that, as mentioned above, a room-temperature volume of HD gas contains significant amounts of hydrogen and deuterium molecules [22], the agreement between the results of the proposed model [14] and the experimental data is more than satisfactory. Additionally, if one takes into account the extremely small volume occupied by the particles injected in the helium bath [21], it can be safely assumed that the steady-state properties of the vortex tangle probed by different particles are the same, that is, our experimental results show that deuterium particles effectively experience a less dense tangle, compared to hydrogen and deuterium hydride probes, i.e., the c values shown in Fig. 3 for the D cases close to the heater should be regarded as conservative estimates of the corresponding ℓ decrease.

The phenomenon can be intuitively explained by saying that, in the same quantum flow, light particles should accelerate on average more than heavy ones [14], that is, the former should be trapped on quantized vortices for shorter times than the latter and consequently probe fewer vortex reconnection events, which would result in less apparent power-law tails of the corresponding velocity distributions [7]. This can indeed justify the fact that the HD flatness trends are less steep than the D ones, in the proximity of the heater, for $R_1 < 1$, that is, D velocity distributions are characterized by wider quantum tails than HD ones, at constant R_1. However, for the bulk cases, H and D flatness trends have similar slopes, that is, our argument apparently suggests that, close to the heater, the distance between quantized vortices deviates from its mean more than in the bulk, which
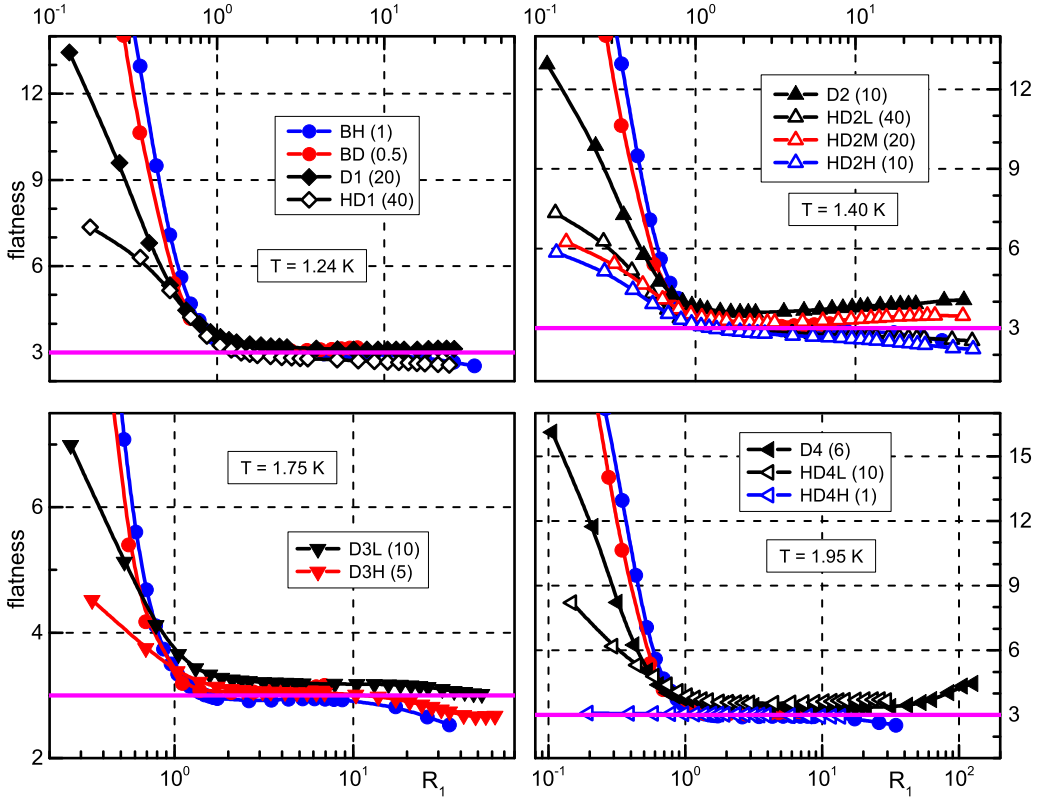
FIG. 4. Flatness of the $(u - u_m)/u_{s.d.}$ distribution as a function of the effective scale ratio $R_1 = cR$ [Eq. (6)]. Relevant c values are shown in parentheses following the data set symbols, which are as in Fig. 1 (see also Table I). Note that, compared to Fig. 3, different scales are used here to highlight the data obtained in the heater proximity.

is another way of saying that the vortex tangle appears to have in the bulk a more regular structure than close to the boundaries.

B. Heat flux and temperature dependences

We now consider the influence on the observed particle dynamics of the applied heat flux. It is evident from Fig. 2 that, at constant temperature, the flatness trends of same-type particles depend on the counterflow velocity and, following the previous reasoning, we can say that these particles, probing flows with increasing v_{ns}, appear to experience less dense vortex tangles. It is indeed known that particles are less likely to be trapped on quantized vortices, i.e., to move at a relatively constant velocity, at large enough heat fluxes [24,33].

It was shown in Ref. [33] that the ratio between the viscous drag force, acting on a particle, and the pressure gradient force, attracting the particle to a quantum vortex core, increases if the heat flux increases (and the temperature decreases), similarly to the experimentally obtained amplitude of the particle accelerations. Consequently, particles probing faster (colder) quantum flows are expected to accelerate on average more than those in slower (warmer) flows and the present velocity results are consistent with this physical picture.

Additionally, it was reported in Ref. [24], that for data obtained in the same channel, at two hydraulic diameters away from the heater, i.e., in the bulk, $v_{ns} \approx V$ for counterflow velocities up to about 2 mm/s, while at larger v_{ns} values the mean particle velocity is lower than the

counterflow velocity, and here, in the flow source proximity, we observe the same behavior, which once again can be explained by taking into account the larger accelerations of particles probing faster (colder) quantum flows. Consequently, as suggested in Ref. [11], the parameter c should, at constant temperature, decrease as the counterflow velocity is increased because at constant R_1 the increase of $v_{ns}V$ could be balanced by the corresponding decrease of c [see Eq. (6)] and this is indeed apparent from the results obtained at 1.40 K (cases HD2L, HD2M, and HD2H) and 1.75 K (D3L and D3H).

At this point it should be easier to understand the reason why we decided to set $c = 1$ for HD4H, which, as shown, e.g., in Fig. 2, is characterized by classical-like flatness values within the entire range of probed scales, i.e., it is evident that in this case it is not possible to access scales smaller than the characteristic length scale of the flow and consequently to estimate directly the corresponding c, as in other cases. However, following the previous argument, it is possible to say that this value should be smaller than the one we obtained for HD4L and larger than 1.

As mentioned in Ref. [11], the observed decrease of the parameter c as the temperature is increased, at approximately constant counterflow velocity, can be related to the fact that γ increases with temperature [26] [see Eq. (6)]. Moreover, we noted above that the ratio between the Stokes drag and the pressure gradient force also decreases if the temperature increases, at constant heat flux [33]. It then follows that same-type particles should be less likely trapped on quantized vortices (and should accelerate more) at lower temperatures if q does not change and, indeed, if we compare the D3L and D4 velocity flatness trends, we obtain for the latter a smaller c value than for the former.

C. Heater proximity

We have just discussed how our experimental results can be explained by taking into account various physical mechanisms, which, in most cases, can actually occur in any type of particle-laden quantum flow, i.e., it is now time to propose possible reasons for the observed vortex line density enhancement in the heater proximity, following Ref. [11]. We first recall that Eq. (3) relates the vortex line density L to the counterflow velocity, which solely depends on temperature and applied heat flux [see Eq. (1)]. The counterflow velocity v_{ns} can then be said to be a global quantity and Eq. (3) is not expected to hold locally. If we take a region of the flow field and measure there the total length of vortex lines, we find that by using the γ values reported in the literature, Eq. (3) is strictly satisfied only if we are far enough from the flow boundaries, as our experimental results neatly demonstrate.

Additionally, it is apparent from Eq. (3) that the vortex line density should increase with temperature, at constant v_{ns}, and consequently our results could be explained by saying that the temperature in the heater proximity is actually larger than the bulk temperature we measure. However, as mentioned above, the characteristic times of the investigated flows are extremely small and we therefore assume here that the fluid temperature does not vary appreciably in the bath. This is also supported by the fact that recent counterflow measurements [34] show that temperature gradients along a square channel of 7-mm sides are solely observed at heat fluxes larger than those considered in the present study, i.e., for q values up to about 1 kW/m^2 the temperature does not seem to change appreciably away from the heater, in the normal fluid flow direction.

However, it has to be kept in mind that the transition to the turbulent state occurs at smaller velocities in larger channels (see, for example, Ref. [24]), i.e., the same heat flux generates, in different-size channels, flows that are not generally expected to share the same features. Consequently, in order to make a more meaningful comparison, we should look at the temperature gradients observed in the smaller channel at larger-q values.

As Varga *et al.* [34] reported that, for $q \approx 2$ kW/m^2, the temperature increase at about four hydraulic diameters away from the heater is a few mK, the assumption that the liquid temperature in the proximity of our heater does not differ significantly from the one in the bulk still holds. Nevertheless, future experiments should be devoted to measure the temperature gradient along the

channel, as a function of bath temperature and applied heat flux, especially because the effect of the channel geometry on the development of quantum flows is yet to be assessed in detail [24].

Moreover, as pointed out in Ref. [11], heat transport mechanisms in thermal counterflow could be related to phenomena occurring in similar flows of viscous fluids, such as in turbulent Rayleigh-Bénard convection [35], but this should solely become apparent at values of applied heat flux larger than those investigated here, at least in the case of our relatively wide channel.

In summary, the above arguments strongly support the view that, in the range of investigated parameters, the vortex line density should be, in the heater proximity, about two orders of magnitude larger than the one in the bulk, at the same temperature and applied heat flux. As detailed in Ref. [11], this experimental finding can be explained following Refs. [17,36], i.e., the observed ℓ decrease could be due to the classical behavior of the He II normal component, which can account for the tendency of quantum vortices to preferentially concentrate in regions of low fluid velocity, and to the heater surface roughness, which may provide pinning and nucleation sites for the vortices.

IV. CONCLUSION

The behavior of relatively small particles suspended in superfluid ^{4}He has been studied experimentally in the case of thermal counterflow, the most common type of He II flow. We showed that the observed flow-induced particle dynamics depends not only on the experimental conditions, temperature and applied heat flux, but also on the type of particles used to probe the flow.

We specifically found that our results can be explained by taking into account the interactions between particles and quantized vortices. On the one hand, when particles are trapped on vortices, they can probe the occurrence of vortex reconnections, which can justify the small-scale power-law tails of the particle velocity distributions [7] and are deemed to be crucial in explaining energy dissipation mechanisms in quantum flows [37–39]. On the other hand, particles are also influenced by the tangle dynamics when they are not trapped, because the velocity field due to quantized vortices can cause particle accelerations [14,33].

It follows that our experimental findings are consistent with the view that particles subjected to frequent changes of velocity are not likely to be trapped on quantized vortices for long times, i.e., they are less suitable to probe the occurrence of vortex reconnections. The outcome is especially evident for thermal counterflow close to the flow source, when the velocity distributions of solid deuterium hydride particles are compared to those of heavier deuterium particles.

Particle dynamics in thermal counterflow appears then to be influenced not only by the tangle properties, determined by the applied heat flux, bath temperature, and boundary proximity of the studied flow region, but also by the particle inertia, which seems to significantly affect the way in which the used probes interact with the vortices. The latter can be considered to be the main result of the work and consequently our experimental study can also be viewed as an invitation to develop adequate theoretical (and/or numerical) models in view of testing the proposed intuitive explanations of the observed particle dynamics.

We also demonstrated that deuterium hydride particles can be successfully employed for the investigation of He II flows, although in the current setup they are generated together with hydrogen and deuterium probes. It would indeed be interesting to produce small enough particles having the same density as the liquid, in order to minimize inertia effects on the particle dynamics, and the present work can also be regarded as a step in this direction. Additionally, we confirmed that, in the heater proximity, quantized vortices appear to be appreciably closer to each other than in the bulk [11] and more importantly we showed that the result is not significantly influenced by the type of particles used, at least in the range of investigated parameters.

The dependence of the observed vortex line density enhancement on the channel geometry is yet to be clarified and, for example, experiments using different-size channels could be performed to address the issue. The flow behavior at higher heat fluxes could also be studied, following, for example, Ref. [32], especially in order to address possible similarities to heat transport mechanisms in turbulent flows of viscous fluids [35].

Our study also demonstrates that the scale-dependent statistical distributions of particle velocities in He II flows can be employed to estimate the mean distance between quantized vortices, once particle inertia effects are suitably taken into account. Indeed, the present method can probe flow regions that are not accessible to the traditional second-sound attenuation technique (see, e.g., Ref. [40] and reference therein).

In summary, we showed that the study of particle dynamics in turbulent flows of He II not only is interesting in its own right, but can also contribute to our understanding of quantum turbulence, especially in view of clarifying its close similarities to and striking differences from turbulent flows of viscous fluids.

ACKNOWLEDGMENTS

[1] W. F. Vinen and J. J. Niemela, Quantum turbulence, J. Low Temp. Phys. **128**, 167 (2002).

[2] L. Skrbek and K. R. Sreenivasan, Developed quantum turbulence and its decay, Phys. Fluids **24**, 011301 (2012).

[3] C. F. Barenghi, L. Skrbek, and K. R. Sreenivasan, Introduction to quantum turbulence, Proc. Natl. Acad. Sci. USA **111**, 4647 (2014).

[4] M. S. Mongiovì, D. Jou, and M. Sciacca, Non-equilibrium thermodynamics, heat transport and thermal waves in laminar and turbulent superfluid helium, Phys. Rep. **726**, 1 (2018).

[5] P. Švančara and M. La Mantia, Flows of liquid ^{4}He due to oscillating grids, J. Fluid Mech. **832**, 578 (2017).

[6] W. Guo, M. La Mantia, D. P. Lathrop, and S. W. Van Sciver, Visualization of two-fluid flows of superfluid helium-4, Proc. Natl. Acad. Sci. USA **111**, 4653 (2014).

[7] M. La Mantia, P. Švančara, D. Duda, and L. Skrbek, Small-scale universality of particle dynamics in quantum turbulence, Phys. Rev. B **94**, 184512 (2016).

[8] L. Biferale, D. Khomenko, V. L'vov, A. Pomyalov, I. Procaccia, and G. Sahoo, Turbulent statistics and intermittency enhancement in coflowing superfluid ^{4}He, Phys. Rev. Fluids **3**, 024605 (2018).

[9] E. Rusaouen, B. Chabaud, J. Salort, and P.-E. Roche, Intermittency of quantum turbulence with superfluid fractions from 0% to 96%, Phys. Fluids **29**, 105108 (2017).

[10] J. Bertolaccini, E. Lévêque, and P.-E. Roche, Disproportionate entrance length in superfluid flows and the puzzle of counterflow instabilities, Phys. Rev. Fluids **2**, 123902 (2017).

[11] P. Hrubcová, P. Švančara, and M. La Mantia, Vorticity enhancement in thermal counterflow of superfluid helium, Phys. Rev. B **97**, 064512 (2018).

[12] S. Yui, M. Tsubota, and H. Kobayashi, Three-Dimensional Coupled Dynamics of the Two-Fluid Model in Superfluid ^{4}He: Deformed Velocity Profile of Normal Fluid in Thermal Counterflow, Phys. Rev. Lett. **120**, 155301 (2018).

[13] Y. A. Sergeev and C. F. Barenghi, Particles-vortex interactions and flow visualization in ^{4}He, J. Low Temp. Phys. **157**, 429 (2009).

[14] M. La Mantia and L. Skrbek, Quantum turbulence visualized by particle dynamics, Phys. Rev. B **90**, 014519 (2014).

[15] M. La Mantia and L. Skrbek, Quantum, or classical turbulence? Europhys. Lett. **105**, 46002 (2014).

[16] M. Mordant, E. Lévêque, and J.-F. Pinton, Experimental and numerical study of the Lagrangian dynamics of high Reynolds turbulence, New J. Phys. **6**, 116 (2004).

[17] M. La Mantia, Particle dynamics in wall-bounded thermal counterflow of superfluid helium, Phys. Fluids **29**, 065102 (2017).

[18] F. Toschi and E. Bodenschatz, Lagrangian properties of particles in turbulence, Annu. Rev. Fluid Mech. **41**, 375 (2009).

[19] M. Bourgoin, J.-F. Pinton, and R. Volk, in *Modeling Atmospheric and Oceanic Flows: Insights from Laboratory Experiments and Numerical Simulations*, edited by T. von Larcher and P. D. Williams (American Geophysical Union, Washington, DC, 2015), p. 277.

[20] O. Bostanjoglo and R. Kleinschmidt, Crystal structure of hydrogen isotopes, J. Chem. Phys. **46**, 2004 (1967).

[21] M. La Mantia, T. V. Chagovets, M. Rotter, and L. Skrbek, Testing the performance of a cryogenic visualization system on thermal counterflow by using hydrogen and deuterium solid tracers, Rev. Sci. Instrum. **83**, 055109 (2012).

[22] H. C. Urey and D. Rittenberg, Some thermodynamic properties of the H^1H^2, H^2H^2 molecules and compounds containing the H^2 atom, J. Chem. Phys. **1**, 137 (1933).

[23] I. F. Sbalzarini and P. Koumoutsakos, Feature point tracking and trajectory analysis for video imaging in cell biology, J. Struct. Biol. **151**, 182 (2005).

[24] M. La Mantia, Particle trajectories in thermal counterflow of superfluid helium in a wide channel of square cross section, Phys. Fluids **28**, 024102 (2016).

[25] R. J. Donnelly and C. F. Barenghi, The observed properties of liquid helium at the saturated vapor pressure, J. Phys. Chem. Ref. Data **27**, 1217 (1998).

[26] S. Babuin, M. Stammeier, E. Varga, M. Rotter, and L. Skrbek, Quantum turbulence of bellows-driven ^{4}He superflow: Steady state, Phys. Rev. B **86**, 134515 (2012).

[27] Y. A. Sergeev, C. F. Barenghi, and D. Kivotides, Motion of micron-size particles in turbulent helium II, Phys. Rev. B **74**, 184506 (2006).

[28] J. T. Tough, in *Progress in Low Temperature Physics*, edited by D. F. Brewer (North-Holland, Amsterdam, 1982), Vol. VIII, p. 133.

[29] K. W. Schwarz, Turbulence in superfluid helium: Steady homogeneous counterflow, Phys. Rev. B **18**, 245 (1978).

[30] K. W. Schwarz, Three-dimensional vortex dynamics in superfluid ^{4}He: Homogeneous superfluid turbulence, Phys. Rev. B **38**, 2398 (1988).

[31] S. W. Van Sciver, *Helium Cryogenics* (Springer, New York, 2012).

[32] E. Varga and L. Skrbek, Dynamics of the density of quantized vortex lines in counterflow turbulence: Experimental investigation, Phys. Rev. B **97**, 064507 (2018).

[33] M. La Mantia, D. Duda, M. Rotter, and L. Skrbek, Lagrangian accelerations of particles in superfluid turbulence, J. Fluid Mech. **717**, R9 (2013).

[34] E. Varga, S. Babuin, V. S. L'vov, A. Pomyalov, and L. Skrbek, Transition to quantum turbulence and streamwise inhomogeneity of vortex tangle in thermal counterflow, J. Low Temp. Phys. **187**, 531 (2017).

[35] F. Chillà and J. Schumacher, New perspectives in turbulent Rayleigh-Bénard convection, Eur. Phys. J. E **35**, 58 (2012).

[36] G. W. Stagg, N. G. Parker, and C. F. Barenghi, Superfluid Boundary Layer, Phys. Rev. Lett. **118**, 135301 (2017).

[37] S. Zuccher, M. Caliari, A. W. Baggaley, and C. F. Barenghi, Quantum vortex reconnections, Phys. Fluids **24**, 125108 (2012).

[38] A. Villois, D. Proment, and G. Krstulovic, Universal and nonuniversal aspects of vortex reconnections in superfluids, Phys. Rev. Fluids **2**, 044701 (2017).

[39] P. Clark di Leoni, P. D. Mininni, and M. E. Brachet, Dual cascade and dissipation mechanisms in helical quantum turbulence, Phys. Rev. A **95**, 053636 (2017).

[40] E. Varga, S. Babuin, and L. Skrbek, Second-sound studies of coflow and counterflow of superfluid ^{4}He in channels, Phys. Fluids **27**, 065101 (2015).